

Bose-Einstein Condensation in solid ^4He

S.O. Diallo,¹ J.V. Pearce,² R.T. Azuah,^{3,4} O. Kirichek,⁵ J.W. Taylor,⁵ and H.R. Glyde¹

¹*Department of Physics and Astronomy, University of Delaware, Newark, Delaware 19716-2593, USA*

²*National Physical Laboratory, Teddington, United Kingdom*

³*NIST Center for Neutron Research, Gaithersburg, Maryland 20899-8562, USA*

⁴*Department of Materials Science and Engineering,*

University of Maryland, College Park, Maryland 20742-2115, USA

⁵*ISIS Spallation Neutron Source, Rutherford Appleton Laboratory, Chilton, Didcot, OX11 0QX, United Kingdom*

(Dated: June 15, 2018)

We present neutron scattering measurements of the atomic momentum distribution, $n(\mathbf{k})$, in solid helium under a pressure $p = 41$ bars and at temperatures between 80 mK and 500 mK. The aim is to determine whether there is Bose-Einstein condensation (BEC) below the critical temperature, $T_c = 200$ mK where a superfluid density has been observed. Assuming BEC appears as a macroscopic occupation of the $k = 0$ state below T_c , we find a condensate fraction of $n_0 = (-0.10 \pm 1.20)\%$ at $T = 80$ mK and $n_0 = (0.08 \pm 0.78)\%$ at $T = 120$ mK, consistent with zero. The shape of $n(\mathbf{k})$ also does not change on crossing T_c within measurement precision.

In 2004, Kim and Chan [1, 2] reported the spectacular observation of a superfluid density in solid helium below a critical temperature, T_c . The superfluid density, ρ_S , is observed as a non-classical rotational inertia (NCRI) in a torsional oscillator (TO) containing solid helium. The percent of solid that has a NCRI and is decoupled from the rest of the solid was $\rho_S(T) \simeq 1.5\%$ at temperature $T = 50$ mK in commercial grade purity ^4He which contains typically 0.3 ppm of ^3He , where $T_c = 200$ mK. All other impurities are frozen out. A ρ_S was observed in both bulk solid helium [2] and in solid confined in porous media (Vycor) [1]. The magnitude of ρ_S varies somewhat from solid sample to solid sample [3]. A superfluid density was observed in solids at pressures between $p \sim 25$ bars near the melting line and 135 bars with ρ_S taking its maximum value of 1.5% at $p \sim 50$ bars.

This remarkable result has been confirmed in independent TO measurements [4, 5, 6]. Rittner and Reppy [5] find that ρ_S can be significantly reduced by annealing the solids near their melting temperatures with ρ_S reduced to zero in some cases. Similarly, Shirahama and coworkers [4] report a reduction in ρ_S of up to 50% by annealing. Macroscopic superflow was not observed in helium in Vycor [7] and bulk helium [8]. However, Sasaki *et al.* [9] have observed macroscopic superflow in those solids which contain grain boundaries that extend across the solid. This unexpected result suggests that there is indeed superflow and that it is along or associated with grain boundaries. Superflow related to grain boundaries [9], the variation of ρ_S from sample to sample [3] and the reduction of ρ_S by annealing [4, 5] suggest that a superfluid density may be associated with macroscopic defects that extend across or whose impact extends across the whole solid.

In liquid helium, Bose-Einstein condensation (BEC) and superfluidity are observed together. Indeed superflow can be shown to follow from BEC [10, 11]. It can also be shown to arise from long range atomic exchanges

[12]. In the liquid, both in bulk [13] and in Vycor [15], BEC is observed as a macroscopic occupation of the $k = 0$ state in $n(\mathbf{k})$, as expected for a translationally invariant system. Solid helium is also translationally invariant, as is a gas of vacancies in the solid. Thus, for certain models of superflow we anticipate that BEC will appear as a macroscopic occupation of $k = 0$ in $n(\mathbf{k})$. In this context we look for an enhancement of $n(\mathbf{k})$ at $k \sim 0$ below T_c . We also look for a change in shape of $n(\mathbf{k})$ below T_c . The central result is that we observe no increase in $n(\mathbf{k})$ at $k \sim 0$ nor any change in shape of $n(\mathbf{k})$ as the temperature is lowered below T_c .

In 1969, Andreev and Lifshitz [16] proposed that helium could be a supersolid if the solid contained vacant sites in the ground state. Essentially, the ground state, zero point vacancies could form a Bose gas at $T \sim 0$ K in which the Bose-Einstein condensate fraction, n_0 , and ρ_S are both approximately 100%. While thermally activated vacancies have been observed [17], ground state vacancies have not. Chester [18] proposed that superflow in solid helium may be possible because the solid is well described by fluid like wave functions that support superflow. Leggett [19] examined superflow via long range exchanges of atoms within a perfect helium solid and found superflow possible but that ρ_S would be small, $\rho_S \sim 0.01\%$.

Recent accurate path integral Monte Carlo calculations [20] find that ρ_S arising from long range atomic exchanges in a perfect crystal will be unobservably small. Similarly, BEC in bulk perfect crystals is predicted to be very small [21, 22]. Zero point vacancies in the ground state are predicted to be unstable [21]. Essentially, vacancies migrate to a surface or coalesce to create a surface and leave the crystal. However, if solid helium is held in an amorphous rather than the equilibrium crystal state, both ρ_S and n_0 take significant values [21]. With these predictions, it is interesting to search for BEC where ρ_S is observed.

The solid ^4He investigated in this experiment was

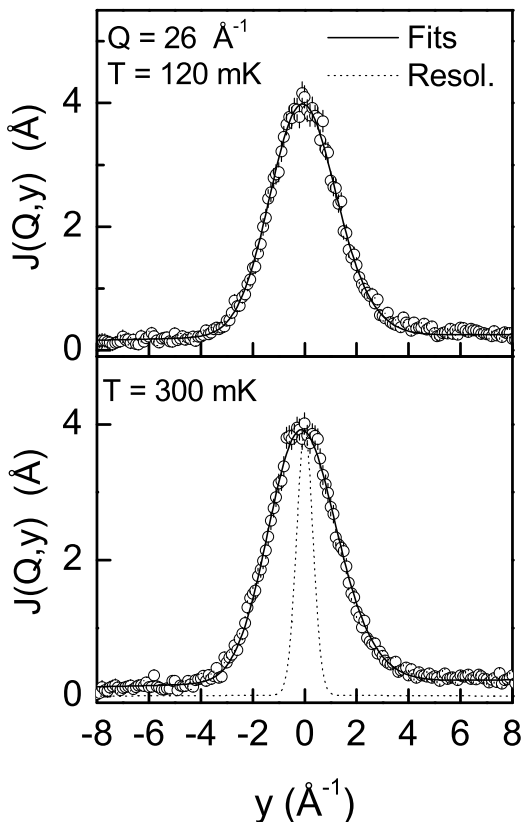


FIG. 1: Observed $J(Q, y)$ of solid ${}^4\text{He}$ at $V = 20.01 \text{ cm}^3/\text{mol}$ (open circles) folded with the instrument resolution at momentum transfer $Q = 26 \text{ \AA}^{-1}$ and temperatures $T = 120$ (top) and 300 mK (bottom). The solid lines are fits of the Convolution Approach (CA) with Final State (FS) function taken from liquid ${}^4\text{He}$ (Ref. [13]), shape of $n(\mathbf{k})$ from Ref. [24] and width $\bar{\alpha}_2$ parameter as the single free fitting parameter. The data peaks below $y = 0$ because of FS effects. The dotted line is the MARI instrument resolution function.

grown using the blocked capillary method. Commercial grade purity ${}^4\text{He}$ (0.3 ppm ${}^3\text{He}$) was introduced into a cylindrical Al sample cell of 20 mm diameter and 62 mm height at a temperature $T \simeq 3$ K to a pressure of $p \simeq 70$ bars. At constant p , the temperature was reduced using an Oxford Instruments Kelvinox VT dilution refrigerator until solid formed in the capillary and blocked the cell. The block was observed at filling $p = (69.8 \pm 0.2)$ bars and $T = (2.79 \pm 0.02)$ K, which corresponds to liquid on the melting line at a molar volume $V_m = (20.01 \pm 0.02) \text{ cm}^3/\text{mol}$ [23]. The blocked cell was further cooled and neutron inelastic scattering measurements at high momentum transfer were made in the solid hcp phase at 80 mK, 120 mK, 300 mK and 500 mK on the MARI spectrometer at the ISIS neutron facility.

Single atom dynamics is observed in the dynamic structure factor $S(Q, \omega)$ at high momentum transfer, $\hbar Q$.

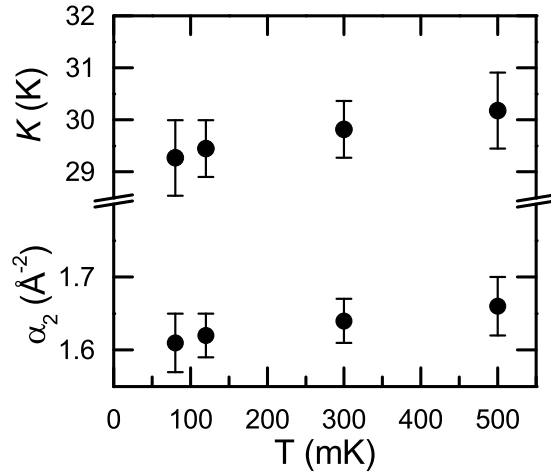


FIG. 2: The mean square atomic momentum, $\bar{\alpha}_2 = \langle k_Q^2 \rangle$ along an axis and the atomic kinetic energy $K = (3\lambda/2)\bar{\alpha}_2$ where $\lambda = 12.12 \text{ K \AA}^2$ of solid helium at $V = 20.01 \text{ cm}^3/\text{mole}$ versus temperature.

Specifically, at $\hbar Q \rightarrow \infty$, where the Impulse Approximation (IA) is valid, the energy transfer $\hbar\omega$ in $S(Q, \omega)$ is Doppler broadened by the atomic momentum distribution $n(\mathbf{k})$. In this limit, it is convenient to express ω in terms of the ‘ y scaling’ wave vector variable, $y = (\omega - \omega_R)/v_R$ where $\omega_R = \hbar Q^2/2m$ and $v_R = \hbar Q/m$, and to present the neutron inelastic data as $J(Q, y) = v_R S(Q, \omega)$. Including final state (FS) effects which are small but not negligible at the Q values investigated here,

$$J(Q, y) = \int dy' R(Q, y - y') J_{IA}(y') \quad (1)$$

where $R(Q, y)$ is the FS broadening function and

$$J_{IA}(y) = \int d\mathbf{k} n(\mathbf{k}) \delta(k_Q - y) = n_Q(y) \quad (2)$$

is the IA to $J(Q, y)$. Specifically, $J_{IA}(y)$ is $n(\mathbf{k})$ projected along \mathbf{Q} denoted the longitudinal momentum distribution [25].

Fig. 1 shows the observed $J(Q, y)$ at wavevectors $Q = 26 \text{ \AA}^{-1}$ and temperatures $T = 120$ mK and $T = 300$ mK. The observed $J(Q, y)$ includes the MARI instrument resolution function which is shown separately as a dotted line in Fig. 1. The solid line is a fit of a model to the data as described below. We were able to determine at most two free parameters in model fits to the data.

To obtain a condensate fraction, we assumed a model $n(\mathbf{k})$ of the form,

$$n(\mathbf{k}) = n_0 \delta(\mathbf{k}) + (1 - n_0) n^*(\mathbf{k}), \quad (3)$$

where $n^*(\mathbf{k})$ is the momentum distribution of the atoms above the condensate in the $k > 0$ states. To proceed, we

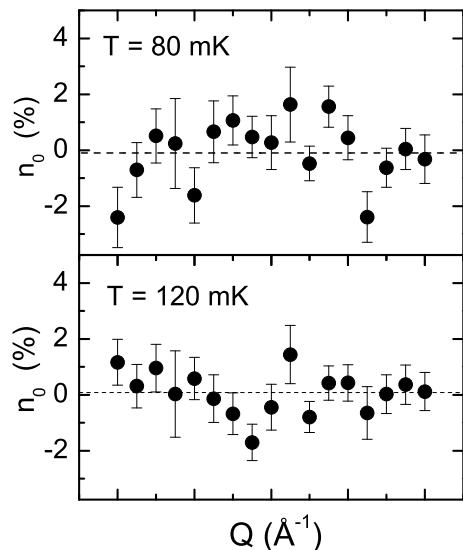


FIG. 3: Condensate fractions obtained by fitting the Convolution Approach (CA) at $T = 80$ mK and 120 mK with the width of $n(\mathbf{k})$ ($\bar{\alpha}_2$) held fixed at its values shown in Fig.2. We find $n_0 = (-0.01 \pm 1.20)\%$ at $T = 80$ mK and $n_0 = (0.08 \pm 0.78)\%$.

assume (1) that the shape of $n(\mathbf{k})$ is the same as observed previously in solid helium at a somewhat lower pressure [24] and (2) that the FS function $R(Q, y)$ in Eq.(1) is the same as observed [13] in liquid helium. The free parameters (two) in the model are then n_0 and the width, $\bar{\alpha}_2$, of the Gaussian component of $n^*(\mathbf{k})$. A condensate component appears as an additional intensity unbroadened by $n^*(\mathbf{k})$ in $J_{IA}(y)$ at $y = 0$.

We first fit the model $n(\mathbf{k})$ to the data at 500, 300, 120 and 80 mK assuming $n_0 = 0$ at all temperatures. The n_0 is expected to be zero at 300 and 500 mK. The resulting values of $\bar{\alpha}_2$ and the associated atomic kinetic energy ($K = (3\hbar^2/2m)\bar{\alpha}_2$) are shown in Fig. 2. The resulting $\bar{\alpha}_2$ and K decrease somewhat with decreasing temperature. In a recent measurement, Adams *et al.* [14] find K independent of temperature within precision.

If superflow is associated with defects in the solid such as vacancies, we anticipate that BEC is similarly associated with these defects, perhaps in a vacancy gas. In this event, the atomic kinetic energy, K , of the majority of the atoms may be largely unaffected by the BEC in the defects. To obtain n_0 at 80 mK and 120 mK within this picture we kept $\bar{\alpha}_2$ fixed at the values obtained above and refitted model (3) with n_0 as a free parameter. The fitted values of n_0 are shown in Fig. 3. The variation of n_0 with Q reflects the statistical error in n_0 . The mean values are $n_0 = (-0.1 \pm 1.2)\%$ at 80 mK and $n_0 = (0.08 \pm 0.78)\%$ at 120 mK.

If, in contrast, the superflow and BEC lie within the bulk of the solid, we anticipate, as in liquid ^4He , that the atomic kinetic energy, K , will decrease below T_c as a result of BEC. The observed decrease in K below T_c has

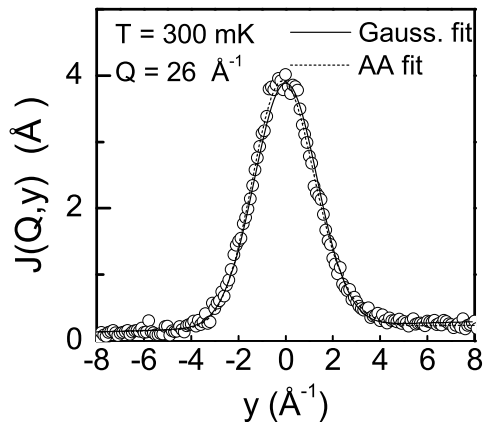


FIG. 4: Fits of the Additive Approach (AA) which includes FS effects and a simple Gaussian to the observed $J(Q, y)$.

been used to estimate n_0 in liquid ^4He [26, 27]. To address this case, we kept $\bar{\alpha}_2$ (kinetic energy arising from $n^*(\mathbf{k})$, constant at the value obtained at 300 mK and refitted model (3) at 80 mK and 120 mK to obtain n_0 . The resulting values are $n_0 = (0.8 \pm 1.2)\%$ at 80 mK and $n_0 = (0.76 \pm 0.77)\%$ at 120 mK. This method assumes that all the drop in K below $T_c = 200$ mK arises from BEC. To normalize these n_0 values for changes in K from other sources, we also determined n_0 at 300 mK. That is, we kept the $\bar{\alpha}_2$ fixed at its 500 mK value and refitted the model to determine n_0 at 300 mK giving $n_0 = (0.63 \pm 0.77)\%$. Since n_0 at 300 mK is zero, we expect the n_0 values below T_c to be overestimated by approximately 0.6%. Normalizing for this overestimate, we arrive at $n_0 \simeq (0.2 \pm 1.2)\%$ at 80 mK and $n_0 \simeq (0.1 \pm 0.8)\%$ at 120 mK. If we try to determine both $\bar{\alpha}_2$ and n_0 simultaneously, we get essentially the same values as before, with only larger error bars; e.g. $n_0 = (0.74 \pm 1.01)\%$ at $T = 120$ mK. Thus all methods give similar values of n_0 .

To investigate a possible change in shape of $J(Q, y)$ or $n(\mathbf{k})$ on crossing $T_c = 200$ mK, we fit the additive approach (AA) [28] to the data. In this model to lowest order, $J(Q, y)$ is [15, 28]

$$J(Q, y) = \left[1 - \frac{\bar{\mu}_3}{2\bar{\alpha}_2^{3/2}} \left(x - \frac{x^3}{3} \right) + \frac{\bar{\mu}_4}{8\bar{\alpha}_2^2} (1 - 2x^2 + \frac{x^4}{3}) \right] J_G(x) \quad (4)$$

where $J_G = \frac{1}{\sqrt{2\pi\bar{\alpha}_2}} \exp(-\frac{x^2}{2})$ and $x = y/\bar{\alpha}_2^{1/2}$. The second term in (4) is the leading FS term and the third term is the leading correction to a Gaussian $n(\mathbf{k})$ plus a FS term. The fitting parameters are $\bar{\alpha}_2$, $\bar{\mu}_3 = \bar{\alpha}_3/\lambda Q$, and $\bar{\mu}_4 = \bar{\alpha}_4 + \bar{\alpha}_4/(\lambda Q)^2$. Previously we found $\bar{\alpha}_4 = 0$ [13, 15, 25]. The three remaining parameters are $\bar{\alpha}_2$, $\bar{\mu}_3$, and $\bar{\alpha}_4$. The kurtosis of $n(\mathbf{k})$ is $\delta = \frac{\bar{\alpha}_4}{\bar{\alpha}_2^2}$.

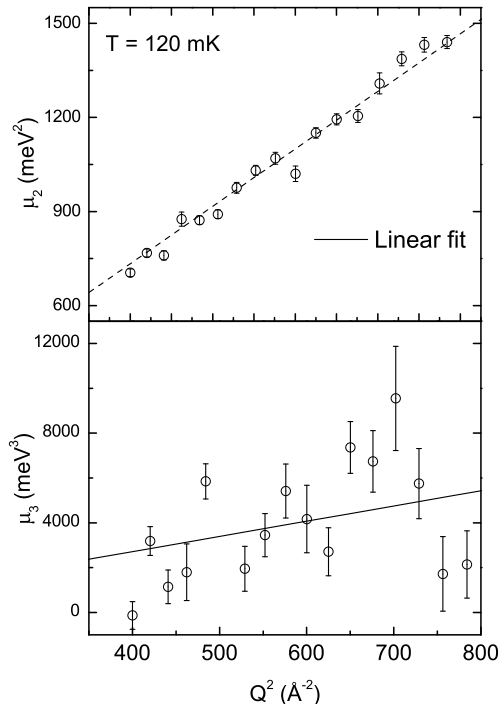


FIG. 5: Fitting parameters $\hbar^2\mu_2 = (\lambda Q)^2 \bar{\alpha}_2$ and $\hbar^3\mu_3 = (\lambda Q)^2 \bar{\alpha}_3$ in the AA giving $\bar{\alpha}_2 = 1.67 \text{ \AA}^{-2}$ and $\bar{\alpha}_3/\lambda = 6.21 \text{ \AA}^{-4}$.

Fig. 4 compares AA and simple Gaussian fits to data. The AA gives a better fit with the peak position lying at $y < 0$ in agreement with the data. We were able to determine only two parameters, e.g. $\hbar^2\mu_2 = (\lambda Q)^2 \bar{\alpha}_2$ and $\hbar^3\mu_3 = (\lambda Q)^2 \bar{\alpha}_3$ where $\lambda = \hbar^2/m = 1.0443 \text{ meV \AA}^2 = 12.12 \text{ K \AA}^2$. These parameters are plotted in Fig. 5 and show the expected Q dependence. We found again a smooth change in $\bar{\alpha}_2$ with temperature as shown in Fig.2 and found $\bar{\alpha}_3/\lambda$ independent of temperature. We tried keeping $\bar{\alpha}_2$ fixed and fitting for $\bar{\mu}_3$ and $\bar{\alpha}_4$ but we were not able to determine $\bar{\alpha}_4$. $\delta = 0$ or $\delta = 0.4$ fit equally well. Thus we find no change in the shape of $J(Q, y)$ or $n(\mathbf{k})$ at T_c within precision.

The condensate fraction, n_0 , of a perfect crystal is expected to be very small [21, 22], $n_0 < 10^{-8}$. In a perfect crystal, BEC requires double occupation of a lattice site which has very high energy and is therefore very improbable. If there are vacant sites, n_0 in the crystal is dramatically increased, to $n_0 \simeq 0.23 \%$ for a vacancy concentration $c_V \simeq 1 \%$ [29]. If the solid is frozen in a non-equilibrium amorphous state, $n_0 \simeq 0.5 \%$ [30]. The n_0 in the amorphous state is relatively insensitive to density although ρ_S decreases significantly with increasing density [30].

If the vacancies are treated as an ideal Bose gas in which $n_0 \simeq 100\%$ and $\rho_S \simeq 100\%$, a vacancy concentration gas $c_V \sim 1.5 \%$ is needed to reach $\rho_S = 1.5 \%$ in the solid.

This also predicts $n_0 \sim 1.5 \%$. This large value of n_0 and this simple model appears to be excluded by our observed values, of $n_0 = (-0.10 \pm 1.20)\%$. In contrast, the n_0 values within bulk solid helium including vacancies [29] or in extended amorphous regions [30], whether in equilibrium or not, are consistent with our observed value.

In summary, we have determined the BEC condensate fraction in commercial grade purity solid helium at pressure 41 bars and molar volume $20.01 \text{ cm}^3/\text{mole}$ using inelastic neutron scattering. We find a condensate fraction $n_0 = (-0.10 \pm 1.20)\%$ below $T_c = 200 \text{ mK}$ consistent with zero. We also find no change in the shape of the atomic momentum distribution on crossing T_c .

-
- [1] E. Kim and M.H.W. Chan. *Nature* **225**, 427 (2004).
 - [2] E. Kim and M.H.W. Chan. *Science* **305**, 1941 (2004).
 - [3] E. Kim and M.H.W. Chan. *Phys. Rev. Lett.* **97**, 115302 (2006).
 - [4] M. Kondo *et al.*, KITP miniprogram, Santa Barbara, CA (2006).
 - [5] A.S.C. Rittner and J.D. Reppy. *Phys. Rev. Lett.* **97**, 165301 (2006).
 - [6] Adrian Choe. *Science* **311**, 1693 (2006).
 - [7] J. Day *et al.*, *Phys. Rev. Lett.* **95**, 035301 (2005).
 - [8] J. Day and J. Beamish. *Phys. Rev. Lett.* **96**, 105304 (2006).
 - [9] S. Sasaki *et al.*, *Science* **313**, 1098 (2006).
 - [10] P. Nozières and D. Pines. *The Theory of Quantum Liquids*. Perseus Books, Cambridge, Massachusetts, (1999).
 - [11] G Baym. in *Mathematical methods in solid state and superfluid theory*, (Eds. R.C. Clark and G.H. Derrick). Oliver and Boyd, Edinburgh (1969).
 - [12] D.M. Ceperley and E.L. Pollock. *Phys. Rev. Lett.* **56**, 351 (1986).
 - [13] H.R. Glyde *et al.*, *Phys. Rev. B* **62** 14337 (2000).
 - [14] M. Adams *et al.*, *in press*, *Phys. Rev. Lett.* (2007)
 - [15] R.T. Azuah *et al.*, *J. Low Temp. Phys.* **130**, 557 (2003).
 - [16] A.F. Andreev and I.M. Lifshitz. *Sov. Phys. JETP* **29**, 1107 (1969).
 - [17] R.O. Simmons. *J. Phys. Chem. Sol.* **55**, 895 (1994).
 - [18] G.V. Chester. *Phys. Rev. A* **2**, 256 (1970).
 - [19] A.J. Leggett. *Phys. Rev. Lett.* **25**, 1543 (1970).
 - [20] D.M. Ceperley and B. Bermu. *Phys. Rev. Lett.* **93**, 155303 (2004).
 - [21] M. Boninsegni *et al.*, *Phys. Rev. Lett.* **97**, 080401 (2006).
 - [22] B.K. Clark and D.M. Ceperley. *Phys. Rev. Lett.* **96**, 105302 (2006).
 - [23] A. Driessen *et al.*, *Phys. Rev. B* **33**, 3269 (1986).
 - [24] S.O. Diallo *et al.*, *Phys. Rev. Lett.* **93**, 075301 (2004).
 - [25] *Momentum Distributions* (Eds. by R.N. Silver and P.E. Sokol). Plenum, New York, (1989).
 - [26] V.F. Sears. *Phys. Rev. B* **28**, 5109 (1983).
 - [27] J. Mayers, C. Andreani, and D. Colognesi. *J. Phys. Condens. Mat.* **9**, 10639 (1997).
 - [28] K.H. Andersen *et al.*, *Phys. Rev. B* **56**, 8978, (1997).
 - [29] D.E. Galli and L. Reatto. *Phys. Rev. Lett.* **96**, 165301 (2006).
 - [30] M. Boninsegni *et al.*, *Phys. Rev. Lett.* **96**, 105301 (2006).